

# Multi-Objective Optimisation of Damper Placement for Improved Seismic Response in Dynamically Similar Adjacent Buildings

Mahesh B. Patil<sup>1</sup>, U. Ramakrishna<sup>2</sup>, and S. C. Mohan<sup>2</sup>

<sup>1</sup>Department of Electrical Engineering, Indian Institute of Technology Bombay

<sup>2</sup>Department of Civil Engineering, BITS Pilani Hyderabad Campus

February 18, 2022

## Abstract

Multi-objective optimisation of damper placement in dynamically symmetric adjacent buildings is considered with identical viscoelastic dampers used for vibration control. First, exhaustive search is used to describe the solution space in terms of various quantities of interest such as maximum top floor displacement, maximum floor acceleration, base shear, and interstorey drift. With the help of examples, it is pointed out that the Pareto fronts in these problems contain a very small number of solutions. The effectiveness of two commonly used multi-objective evolutionary algorithms, viz., NSGA-II and MOPSO, is evaluated for a specific example.

## 1 Introduction

The use of energy dissipation devices to reduce structural vibrations arising due to earthquake excitations has been reported extensively (see [1] for a review). The effect of damper placement as well as damper parameters has been studied in detail. The techniques used for the above purpose can be broadly divided into two categories: (a) parametric study [2]-[4] in which damper parameters or positions are varied in a systematic manner and their effect on the response of interest obtained, (b) optimisation of damper parameters and/or positions with respect to one or more objective functions [5]-[23].

In this paper, we consider a specific case, viz., reduction of seismic response for two dynamically similar adjacent buildings (DSABs) on a rigid foundation using viscoelastic dampers [2],[3], as shown in Fig. 1. Each dashed line in Fig. 1(c) corresponds to two dampers (at either end, as shown in Fig. 1(b)). The equation of motion can be written in the following form [3]:

$$\mathbf{M}\ddot{\mathbf{X}} + (\mathbf{C} + \mathbf{C}_D)\dot{\mathbf{X}} + \mathbf{K}\mathbf{X} = -\mathbf{M}\mathbf{I}\ddot{x}_g. \quad (1)$$

A detailed description of Eq. 1 is given in [3]. The vector  $\mathbf{X}$  contains the relative displacement of each floor (in each of the two buildings) due to the ground acceleration excitation given by  $\ddot{x}_g$ . Throughout this

paper, we have considered the 1940 El Centro ground acceleration.

Eq. 1 is solved using Newmark's method [24] to yield  $\mathbf{X}(t)$ ,  $\dot{\mathbf{X}}(t)$ , and  $\ddot{\mathbf{X}}(t)$ , i.e., the displacements, velocities, and accelerations of all floors of the left and right buildings. The parameters used in this calculation (and also in the rest of the paper) are as follows. The dimensions are as shown in Fig. 1. The mass and stiffness are 64,719 Kg and  $3.7774 \times 10^8$  N/m per storey. The VE damper properties are  $K_d = 10^6$  N/m,  $C_d = 10^8$  N-m/sec.

The top left floor displacement  $x_L(t)$  obtained by solving Eq. 1 for six-storeyed DSABs is shown in Fig. 2(a) when no dampers are used. Fig. 2(b) shows  $x_L(t)$  for the same DSABs but with two dampers connected as shown in the figure. The reduction obtained in  $x_L(t)$  with the use of dampers is clearly seen.

There are several other possible locations for the dampers. The question which naturally arises is whether there is an optimum placement which would lead to smaller displacements (or improved values for any other objective functions). Specifically, in this paper, we consider optimisation of the damper configuration for a given number of floors ( $N_f$ ) and a given number of dampers ( $N_d$ ) with the building and damper parameters, as described above, held constant.

This paper is organised as follows. In Sec. 2, we describe the solution space for specific examples. In Sec. 3, we discuss the formulation of the multi-objective optimisation problem considered in this work and present results obtained for DSABs with  $N_f = 10$  (ten storeys) and different values of  $N_d$ . In Sec. 4, we compare the performance of two commonly used multi-objective evolutionary algorithms (MOEAs), viz, NSGA-II [25] and MOPSO [26] in the context of the damper placement optimisation problem. Finally, in Sec. 5, we present conclusions of this work along with some future research directions.

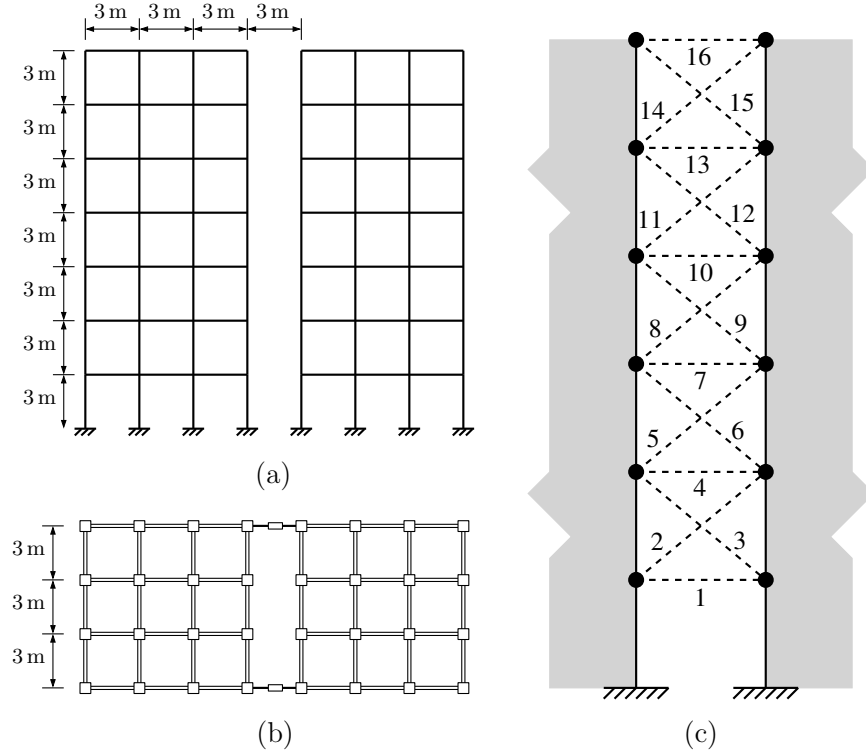


Figure 1: Two dynamically similar adjacent buildings: (a) Elevation, (b) plan, (c) schematic representation.

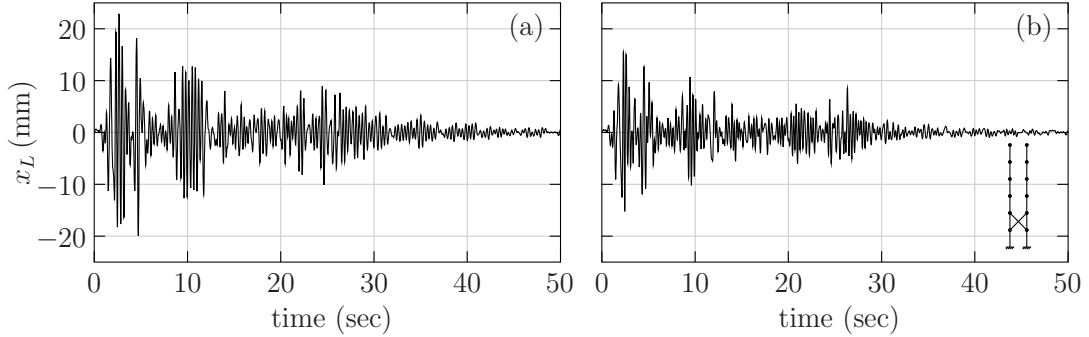


Figure 2: Displacement of top left floor versus time for six-storeyed DSABs as obtained by solving Eq. 1. (a) without dampers, (b) with dampers connected as shown in the inset.

## 2 Solution space examples

The solution space for a multi-objective optimisation problem depends on the choice of the objective functions. For the damper placement optimisation problem, various objective functions have been used in the literature [15]. Here, we describe the solution space for three sets of objective functions for six-storeyed DSABs (i.e.,  $N_f = 6$ ) with two or three dampers (i.e.,  $N_d = 3$  or  $N_d = 4$ ).

### 2.1 Maximum floor displacements

In this case, we consider two objective functions, viz., the maximum displacements (over time) of the top left floor and the top right floor, denoted by  $x_L$  and  $x_R$ , respectively. Figs. 3(a) and 3(b) show the solution space (i.e., solutions obtained for all possible

damper configurations) for  $N_d = 3$  and  $N_d = 4$ . The Pareto-optimal solutions are marked with squares. Since the two buildings are dynamically similar, the  $x_L$  and  $x_R$  values are symmetrically located, as seen in the figure. Figs. 3(c) and 3(d) show the damper configurations corresponding to the Pareto-optimal solutions.

The total number of possible damper positions for  $N_f = 6$  is  $N_f + 2(N_f - 1) = 16$ , as shown in Fig. 1(c), and the total number of damper configurations with  $N_d = 3$  is [13]  ${}^{16}C_3 = 560$ . The solution space in Fig. 3(a) has been obtained by solving Eq. 1 for each of these 560 configurations and recording  $x_L$  and  $x_R$  in each case. It may be noted that some of the  $(x_L, x_R)$  values would overlap, and therefore the number of distinct solutions in Fig. 3(a) would be less than  ${}^{16}C_3$ . Once the entire solution space is found, it is a straightforward matter

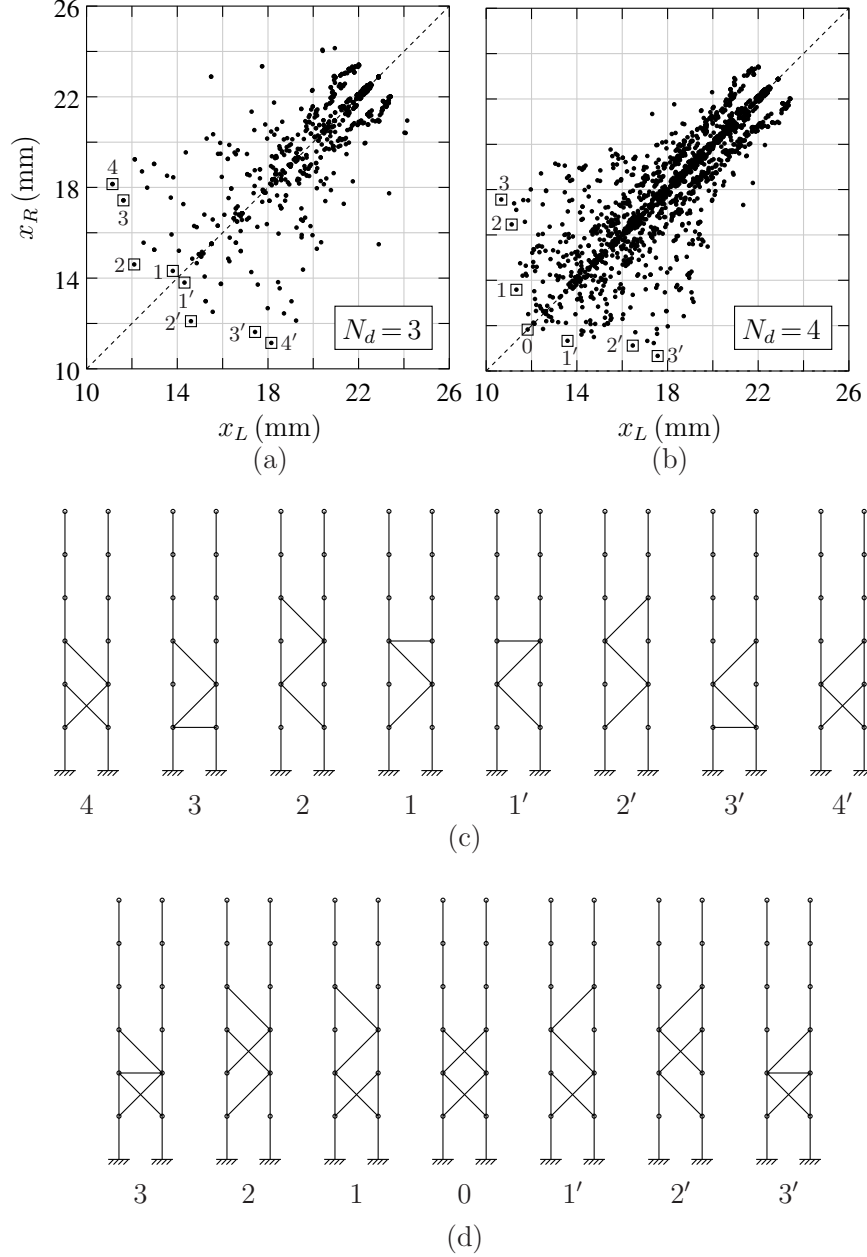


Figure 3: Maximum top left floor and top right floor displacements for six-storeyed DSABs. (a) solutions space for  $N_d = 3$ , (b) solutions space for  $N_d = 4$ , (c) damper placement for Pareto-optimal solutions with  $N_d = 3$ , (d) damper placement for Pareto-optimal solutions with  $N_d = 4$ .

to compare the solutions with each other to obtain the Pareto front.

When the number of possible configurations becomes much larger, it would take too long to evaluate all of them. Furthermore, as  $N_f$  increases, the matrix sizes in Eq. 1 also increase, which means that the solution time per configuration is also larger. For this reason, the above “enumeration” or “exhaustive search” [13] procedure becomes impractical for many cases of practical interest. In this scenario, MOEAs – which would generally require a much smaller number of function evaluations – provide an attractive alternative.

## 2.2 Maximum acceleration and interstorey drift

We now consider another set of two objective functions, viz., the maximum acceleration  $a^{\max}$  and the maximum interstorey drift [14]  $\Delta^{\max}$  (over all floors and time). Figs. 4 (a) and 4 (b) show the solutions space for  $N_d = 3$  and  $N_d = 4$ , respectively. The damper configurations corresponding to the Pareto-optimal solutions are shown Figs. 4 (c) and 4 (d).

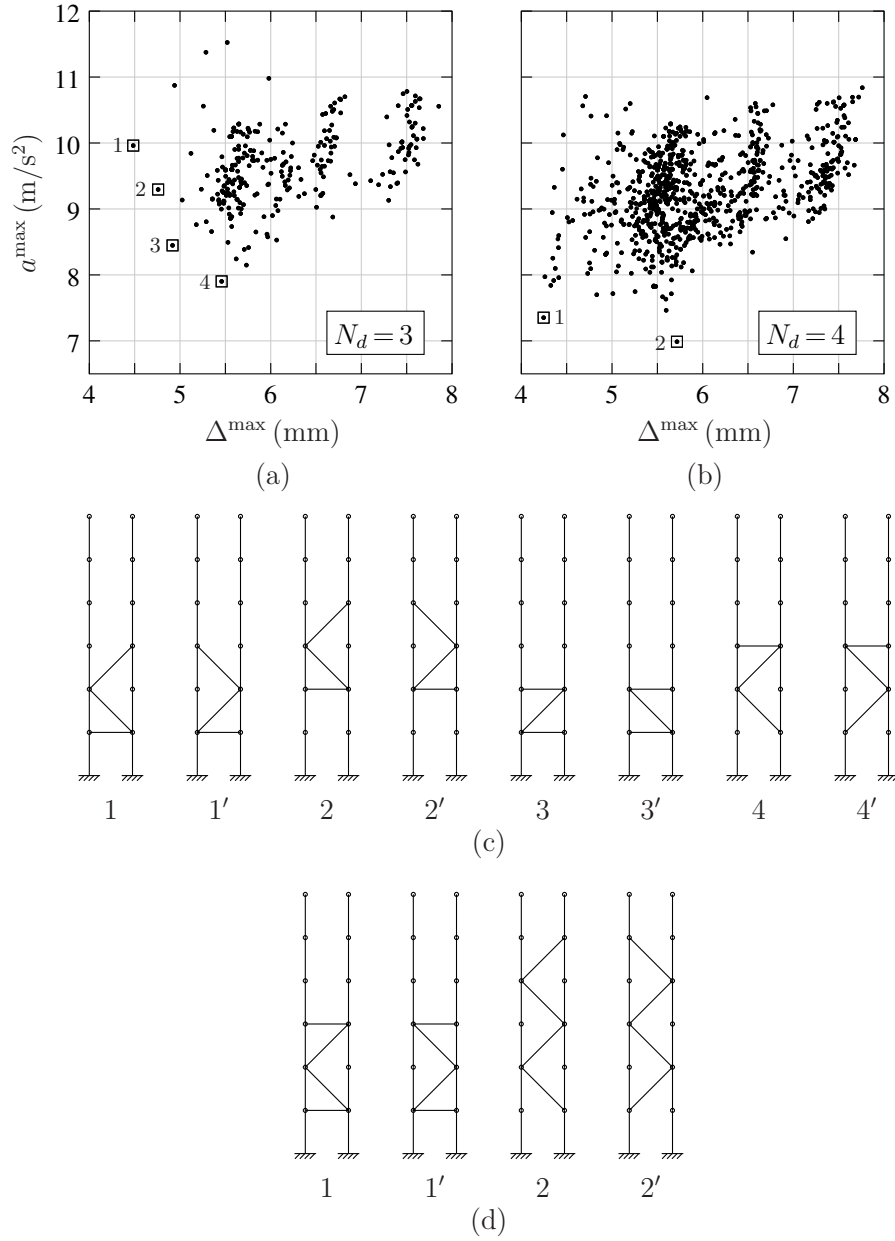


Figure 4: Maximum acceleration and maximum interstorey drift (over all floors and time) for six-storeyed DSABs. (a) solutions space for  $N_d = 3$ , (b) solutions space for  $N_d = 4$ , (c) damper placement for Pareto-optimal solutions with  $N_d = 3$ , (d) damper placement for Pareto-optimal solutions with  $N_d = 4$ .

### 2.3 Maximum top-floor displacement and base shear

The maximum base shear is yet another quantity of interest [2]. The solution space, with the maximum top-floor displacement (over all floors and time) and the maximum base shear (over time) as the two objectives, is shown in Figs. 5(a) and 5(b) for the same  $N_f$  and  $N_d$  values as before. The damper configurations corresponding to the Pareto-optimal solutions are shown in Figs. 5(c) and 5(d).

From Figs. 3-5, we observe that the three Pareto fronts have some damper configurations in common.

For example, configurations 1 and 1' of Fig. 3(c) also appear in Figs. 4(c) and 5(c). However, there are other configurations which do not appear in all three Pareto fronts.

The most striking feature of the solution spaces shown in Figs. 3-5 is the very small number of solutions in the Pareto front. Typically, the performance of an MOEA is evaluated with measures such as generational distance, error ratio, and spread [27]. For the damper placement optimisation problem considered here, these measures are clearly not applicable. Instead, the most relevant performance measure for this problem is the number of times the MOEA is able to obtain the Pareto-optimal

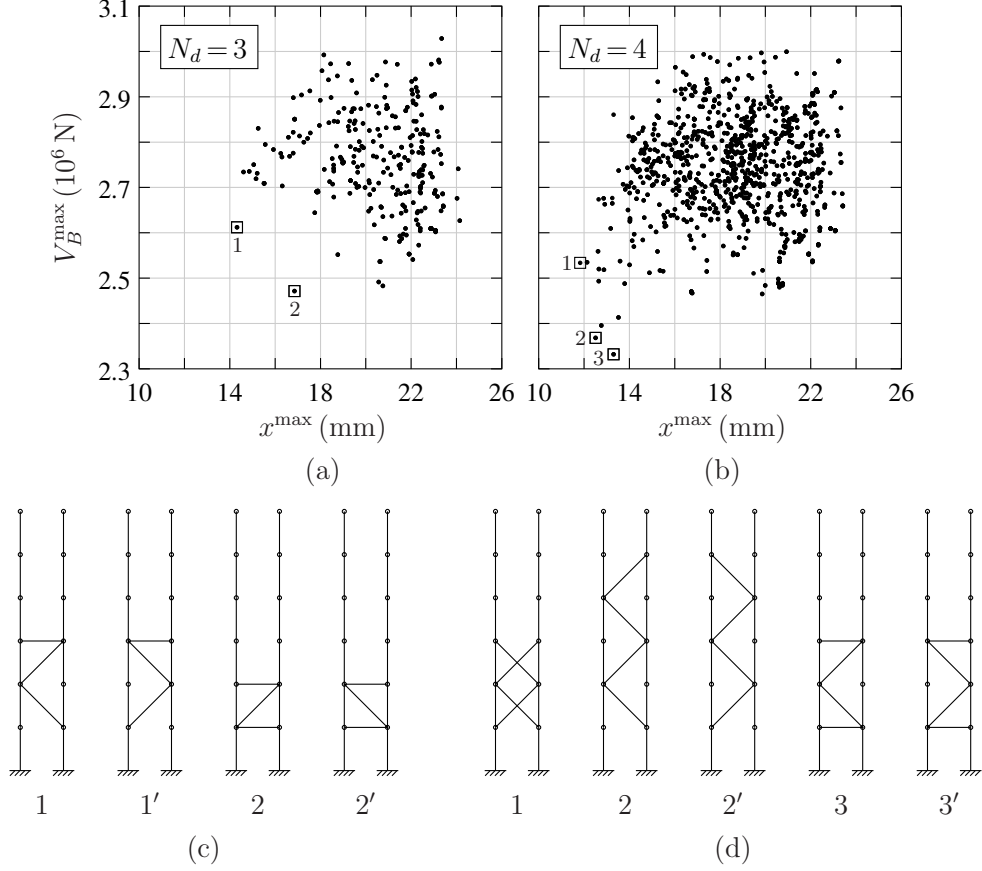


Figure 5: Maximum top-floor displacement (over all floors and time) and maximum base shear (over time) for six-storeyed DSABs. (a) solutions space for  $N_d=3$ , (b) solutions space for  $N_d=4$ , (c) damper placement for Pareto-optimal solutions with  $N_d=3$ , (d) damper placement for Pareto-optimal solutions with  $N_d=4$ .

solutions in a given number of independent runs. We will quantify this performance measure in terms of the “success rate” (SR) for the  $k^{\text{th}}$  Pareto-optimal solution as

$$SR(k) = \frac{N_k}{N_r}, \quad (2)$$

where  $N_r$  is the number of independent runs (trials) of the MOEA, and  $N_k$  is the number of runs in which the  $k^{\text{th}}$  Pareto-optimal solution was obtained. We will use the above definition to compare MOEAs with respect to the damper placement problem in Sec. 4.

### 3 Problem formulation

The multi-objective optimisation problem considered in this paper can be stated as follows. Given two DSABs with  $N_f$  floors and  $N_d$  identical dampers, find the Pareto-optimal set of solutions (damper configurations) with the objectives of minimising  $f_1$  and  $f_2$ . We consider two sets of  $(f_1, f_2)$ :

- (i)  $f_1$  is the maximum interstorey drift ( $\Delta^{\max}$ ), and  $f_2$  is the maximum acceleration ( $a^{\max}$ ), where  $\Delta^{\max}$  and  $a^{\max}$  are maximum values over time

and over all floors. As shown in [12], these two objectives are conflicting in nature, thus making it a multi-objective optimisation problem.

- (ii)  $f_1$  is the maximum top-floor displacement ( $x^{\max}$ ), and  $f_2$  is the maximum base shear [2] ( $V_B^{\max}$ ), where  $x^{\max}$  and  $V_B^{\max}$  are maximum values over time.

Note that several other objective functions have been used in the literature [15]. Here, we have selected two representative sets of objectives. Our main focus is on the optimisation issues involved, and the conclusions drawn from this work are expected to be broadly applicable for other choices of objective functions as well.

Applying an MOEA to the above problem involves repeated evaluation of the objective functions for specific damper configurations. If the NSGA-II algorithm [25] is used, each chromosome in the population would correspond to a specific damper configuration. As an example, consider the damper configuration shown in Fig. 6(a). Treating each damper position  $d_k$  as a decision variable, the chromosome representing this configuration would be characterised by  $d_1=2$ ,  $d_2=4$ ,  $d_3=7$ . Similarly, if the multi-objective particle swarm optimisation (MOPSO) algorithm [26] is used, the

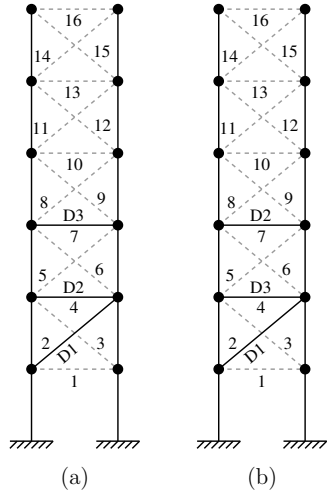


Figure 6: Damper configuration examples for  $N_f=6$ ,  $N_d=3$ .

particle representing the configuration in Fig. 6 (a) would have three parameters, viz.,  $d_1=2$ ,  $d_2=4$ ,  $d_3=7$ .

Since we have assumed the three dampers to have identical properties, the configurations in Figs. 6 (a) and 6 (b) would give the same objective function values although their decision variable values differ ( $d_1=2$ ,  $d_2=4$ ,  $d_3=7$  in Fig. 6 (a), and  $d_1=2$ ,  $d_2=7$ ,  $d_3=4$  in Fig. 6 (b)). Clearly, it is wasteful to evaluate both of these configurations. In order to avoid such repetitive computations, we evaluate a chromosome (or particle) only if the damper positions satisfy  $d_3 > d_2 > d_1$ . If this condition is not satisfied, we assign suitably large values (“penalties”) to the objective functions  $f_1$  and  $f_2$ , thus making that solution unfit.

Another feature which can be used to limit the search space is the following. For  $N_f=6$  and  $N_d=3$ , there are a total of 16 possible damper positions, as shown in Fig. 1 (c). The first position cannot be occupied by D2 or D3 since D1 needs to occupy a position lower than D2. Similarly, the 16<sup>th</sup> position in the figure cannot be occupied by D1 or D2 since D3 needs to occupy a position higher than D2. With this logic, we can limit the search space by restricting the decision variables as

$$d_1 \in \{1, 2, \dots, 13, 14\}, \quad (3)$$

$$d_2 \in \{2, 3, \dots, 14, 15\}, \quad (4)$$

$$d_3 \in \{3, 4, \dots, 15, 16\}.$$

Although the decision variables ( $d_k$ ) in our problem take on only integer values, we consider them as real variables and convert them to integers before evaluating the objective functions. We will describe further details of the algorithms used in this work in Sec. 4.

We now look at the Pareto-optimal solutions obtained for  $N_f=10$  with different values of  $N_d$ . Fig. 7 shows the objective function values for the first set of objectives, i.e.,  $(\Delta^{\max}, a^{\max})$ , for the Pareto-optimal solutions for  $N_d=2$ ,

Table 1: Pareto-optimal solutions for the  $(\Delta^{\max}, a^{\max})$  optimisation problem, with  $N_f=10$  and  $N_d=2, 4, 6$ . Numbers in the index column correspond to the damper configurations shown in Fig. 7.

$N_d$	index	$\Delta^{\max}$ (mm)	$a^{\max}$ (m/s <sup>2</sup> )
2	1	11.52	11.10
4	1	9.52	9.84
	2, 2'	10.42	9.64
	3, 3'	10.59	9.08
	4, 4'	11.20	9.04
6	1	8.16	8.60
	2, 3	8.25	7.89

3, 4, 5, 6, and the damper configurations for  $N_d=2, 4, 6$ . The objective function values for  $N_d=2, 4, 6$  are also listed in Table 1. We observe that, as the number of dampers increases, there is an overall improvement in the objective function values. From Table 1, it is also clear that the two objectives,  $a^{\max}$  and  $\Delta^{\max}$ , are conflicting. As a result, the best configuration for minimum  $a^{\max}$  is in general different than that for minimum  $\Delta^{\max}$ , the only exception being the  $N_d=2$  case.

From Fig. 7, we observe that the optimum configurations take various geometric forms, thus making it difficult to generalise. The complexity would increase further as more objective functions are considered or additional decision variables, such as damper properties, are allowed. For this reason, the use of MOEAs is the only practical option for choosing a damper configuration when the solution space is large.

The Pareto-optimal objective function values for the second set, i.e.,  $(x^{\max}, V_B^{\max})$ , are shown in Fig. 8. The optimal damper configurations for  $N_d=2, 4, 6$  are also shown in the figure, and the corresponding objective function values are listed in Table 2. For these three cases, the configuration which results in minimum  $x^{\max}$  also gives the minimum  $V_B^{\max}$ . These “criss-cross” configurations also appear in the Pareto-optimal sets for the first objective set (Fig. 7) and have been found to be beneficial in the study presented in [3] as well.

## 4 Comparison of MOEAs

As the solutions space grows, the efficiency of the MOEA becomes more important. Let us take a specific example, viz.,  $N_f=10$ ,  $N_d=6$ . In this case, the total number of possible damper positions is  $N_f+2(N_f-1)=28$ , and the size of the solution space  $S$  (defined as the total number of damper configurations) is  ${}^{28}C_6=376,740$ . The average CPU time required for evaluating one configuration was found to be about 6.6 msec on a desktop computer (Linux) with 3.8 GHz clock and 8 GB RAM without any

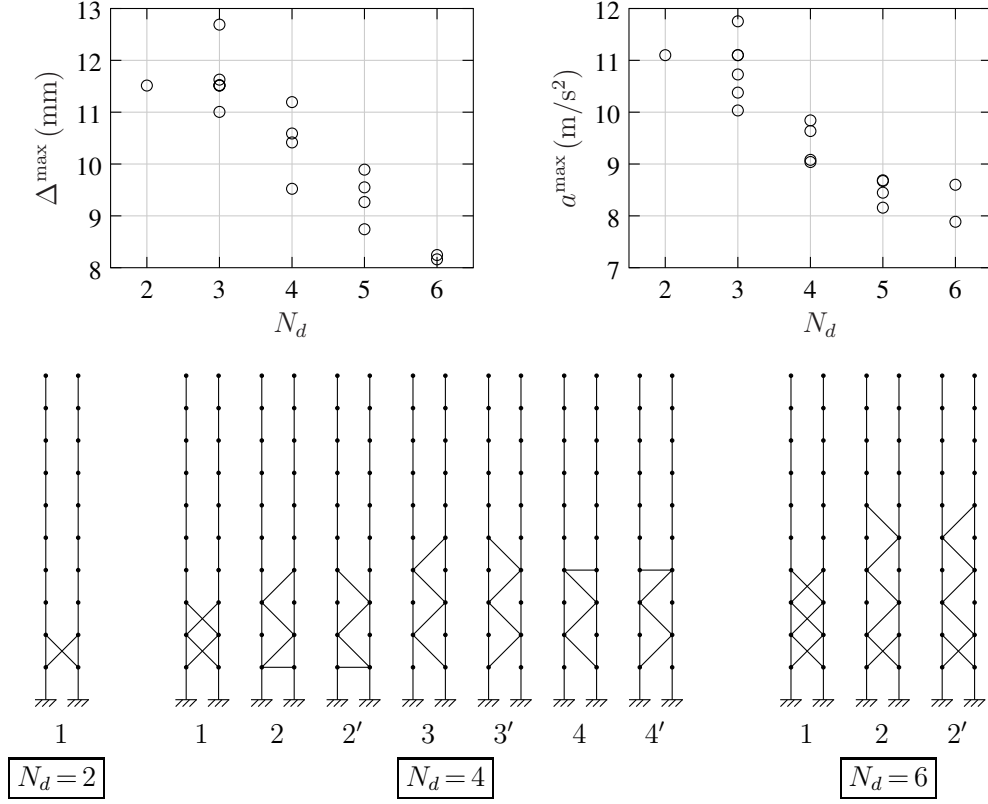


Figure 7: Objective function values for Pareto-optimal solutions of the  $(\Delta^{\max}, a^{\max})$  optimisation problem for different values of  $N_d$ , and optimal damper configurations for  $N_d = 2, 4, 6$ .

Table 2: Pareto-optimal solutions for the  $(x^{\max}, V_B^{\max})$  optimisation problem, with  $N_f = 10$  and  $N_d = 2, 4, 6$ . Numbers in the index column correspond to the damper configurations shown in Fig. 8.

$N_d$	index	$x^{\max}$ (mm)	$V_B^{\max}$ (10 <sup>6</sup> N)
2	1	64.31	5.21
4	1	46.92	4.31
6	1	36.43	3.81

parallelization. Exhaustive search, i.e., evaluation of all possible configurations, would take  $376,740 \times 6$  msec or about 41 minutes. With large values of  $N_f$  or  $N_d$ , the exhaustive search option becomes too expensive, and therefore an MOEA, which can obtain the Pareto front solutions by evaluating a small fraction of  $S$ , is certainly desirable. With this in mind, we define the following two figures of merit for an MOEA in the context of damper placement optimisation for DSABs.

- (a) Computational effort  $CE = \frac{N_{FE}^{\text{total}}}{S}$ , where  $N_{FE}^{\text{total}}$  is the total number of function evaluations carried out by the MOEA in  $N_r$  independent runs, and  $S$  is the size of the solution space. Note that exhaustive

search, which gives all Pareto-optimal solutions, requires  $CE = 1$ . An MOEA which requires  $CE > 1$  for obtaining all Pareto-optimal solutions is therefore of no practical use.

- (b) Success rate  $SR(k)$ , as defined by Eq. 2. An ideal MOEA would find all Pareto-optimal solutions in each run, thus giving  $SR(k) = 1$  for each value of  $k$ , i.e., for each Pareto-optimal solution. In practice,  $SR(k)$  would be smaller.

With the above definitions, we can now compare MOEAs with each other. For the same  $CE$ , an MOEA with a larger  $SR(k)$  is better. Similarly, for the same  $SR(k)$ , an MOEA with a smaller  $CE$  is better. In the following, we will consider the damper placement problem with  $N_f = 10$  and  $N_d = 6$ , and compare the performance of three MOEAs, as described below.

- (a) NSGA-II: This is the real-coded nondominated sorting genetic algorithm presented in [25]. The following algorithm parameters were chosen: crossover probability  $p_c = 0.9$ , distribution index for crossover  $\eta_c = 15$ , mutation probability  $p_{\text{mut}} = 1/L$  (where  $L = N_d$  is the number of decision variables), and distribution index for mutation  $\eta_m = 7$ . Since  $p_{\text{mut}} = 1/N_d$ , on average, one of the damper positions of a given chromosome get mutated. The following polynomial probability distribution is used for

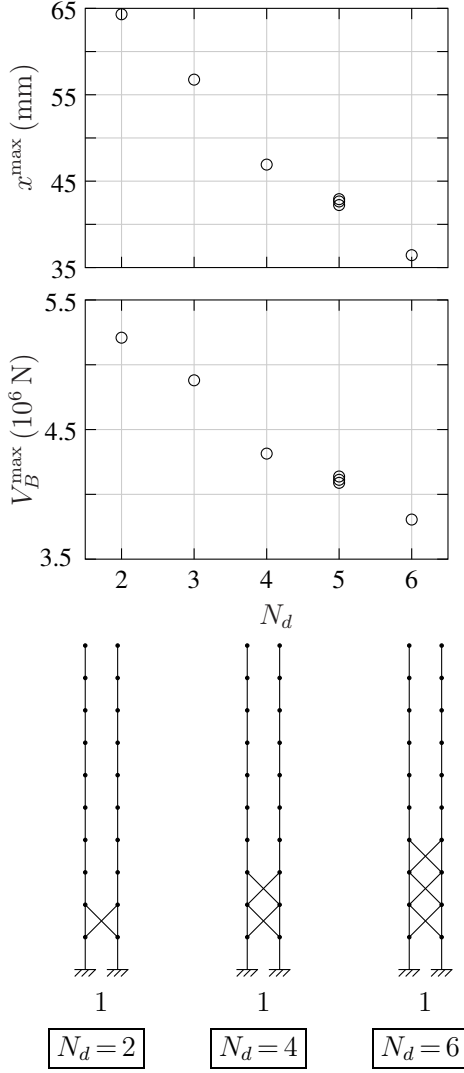


Figure 8: Objective function values for Pareto-optimal solutions of the  $(x^{\max}, V_B^{\max})$  optimisation problem for different values of  $N_d$ , and optimal damper configurations for  $N_d = 2, 4, 6$ .

finding the mutated parameter value [25].

$$P(\delta) = 0.5 (\eta_m + 1) (1 - |\delta|)^{\eta_m}. \quad (5)$$

Eq. 5 ensures that the new (mutated) parameter value is close to the previous value.

- (b) MOPSO-1: This is the same as the MOPSO algorithm described in [26]. The algorithm parameters used in this work are  $W=0.4$ ,  $C_1=2$ ,  $C_2=2$ . As described in [26], the mutation operator is implemented as follows. For example, consider a constant probability of mutation  $p_{\text{mut}}=0.05$ . In this case, in each PSO iteration, 5% of the particles (on average) are randomly selected, and for each of them, one of the parameters, i.e., the position of one of the  $N_d$  dampers, is randomly mutated.
- (c) MOPSO-2: This is identical to MOPSO-1 except for

the implementation of the mutation operation. In MOPSO-2, for each particle selected for mutation, one of the parameters is mutated, as in MOPSO-1. However, instead of mutating it randomly, the polynomial probability distribution given by Eq. 5 is used, with  $\eta_m=7$ .

Several choices exist for the algorithm parameters (such as  $p_c$ ,  $\eta_c$ ,  $\eta_m$  for NSGA-II and  $W$ ,  $C_1$ ,  $C_2$  for MOPSO). Here, we have selected parameter values which have been found to be effective in the literature. Apart from the algorithm parameters, the population size  $N_p$  (number of chromosomes in NSGA-II or number of particles in MOPSO), the number of iterations  $N_{\text{iter}}$ , and the number of independent runs  $N_r$  also play a role in the performance of an MOEA (e.g., see [26]). In this work, we have varied  $N_p$ ,  $N_{\text{iter}}$ ,  $N_r$ , and recorded the performance measures in each case. The results are shown in Tables 3 and 4 for the  $(\Delta^{\max}, a^{\max})$  and  $(x^{\max}, V_B^{\max})$  optimisation problems, respectively. Note that there are three success rates in Table 3, corresponding to the three Pareto-optimal solutions shown in Fig. 7 ( $N_d=6$  case). For example, for the MOPSO-1 algorithm with  $N_p=40$ ,  $N_{\text{iter}}=200$ ,  $N_r=30$ ,  $SR(1)=4/30$ , indicating that solution 1 has been found 4 times in 30 independent runs.

We can make the following observations from Tables 3 and 4.

- (a) The NSGA-II algorithm consistently misses out one of the solutions in Table 3 even with  $CE > 1$ .
- (b) From the first two rows of the NSGA-II section and the first two rows of the MOPSO-1 section of Table 3, we find that the success rate of NSGA-II has not changed significantly by doubling  $N_{\text{iter}}$  whereas that of MOPSO-1 has improved.
- (c) Compared to NSGA-II, the MOPSO algorithm is generally more effective in obtaining all Pareto-optimal solutions. This observation is similar to that in [19] for a different optimisation problem.
- (d) MOPSO-2, which involves the polynomial mutation operator, performs better than MOPSO-1. However, when the mutation probability  $p_{\text{mut}}$  is increased from 0.05 to 0.2, it fails to capture one of the three solutions in Table 3 and the only solution in Table 4.

The above discussion brings out the need for trying out different MOEAs, possibly with some suitable changes incorporated in the algorithms, for solving a given practical multi-objective optimisation problem. In the literature, generally algorithms are evaluated for certain test cases, and results are compared with other algorithms. Results of this work suggest that different problems may require different algorithmic options to be explored for improved efficiency.



Table 3: Summary of performance of NSGA-II, MOPSO-1, and MOPSO-2 algorithms for the  $(\Delta^{\max}, a^{\max})$  optimisation problem, with  $N_f = 10$  and  $N_d = 6$ .

Algorithm	$N_p$	$N_{\text{iter}}$	$N_r$	$P_{\text{mut}}$	CE	SR (1)	SR (2)	SR (3)
NSGA-II	40	200	30	$1/N_d$	0.637	0/30	2/30	4/30
	40	400	30	$1/N_d$	1.274	0/30	2/30	5/30
	100	60	10	$1/N_d$	0.159	0/10	1/10	3/10
	100	120	10	$1/N_d$	0.319	0/10	1/10	4/10
MOPSO-1	40	200	30	0.05	0.637	4/30	4/30	6/30
	40	400	30	0.05	1.274	4/30	5/30	9/30
	40	200	30	0.20	0.637	3/30	9/30	11/30
	40	400	30	0.20	1.274	4/30	9/30	13/30
MOPSO-2	100	60	10	0.05	0.159	2/10	1/10	3/10
	100	60	10	0.20	0.159	0/10	3/10	5/10

Table 4: Summary of performance of NSGA-II, MOPSO-1, and MOPSO-2 algorithms for the  $(x^{\max}, V_B^{\max})$  optimisation problem, with  $N_f = 10$  and  $N_d = 6$ .

Algorithm	$N_p$	$N_{\text{iter}}$	$N_r$	$P_{\text{mut}}$	CE	SR (1)
NSGA-II	40	200	30	$1/N_d$	0.637	0/30
	40	400	30	$1/N_d$	1.274	3/30
	100	60	10	$1/N_d$	0.159	0/10
	100	120	10	$1/N_d$	0.319	0/10
MOPSO-1	40	200	30	0.05	0.637	3/30
	40	400	30	0.05	1.274	3/30
	40	200	30	0.20	0.637	4/30
	40	400	30	0.20	1.274	6/30
MOPSO-2	100	60	10	0.05	0.159	3/10
	100	60	10	0.20	0.159	0/10

## 5 Conclusions

Multi-objective optimisation of viscoelastic damper placement in DSABs is presented. For six-storeyed DSABs with three and four dampers, the complete solution spaces have been obtained for three sets of objectives. In all three cases, it is shown that the number of solutions in the Pareto front is very small. It is argued that, for the DSAB damper placement problem, the figures of merit commonly used for evaluating MOEAs are not meaningful. Two other figures of merit, viz., computational effort and success rate, are therefore used in this work. For ten-storeyed DSABs, optimum damper configurations have been obtained for different values of  $N_d$ , the number of dampers. From the results obtained, it is concluded that the use of MOEAs is the only effective way of obtaining optimum damper placements when the solution space is large.

The performance of two commonly used MOEAs, viz., NSGA-II and MOPSO, is compared in the context of the DSAB damper placement problem. The MOPSO algorithm with a polynomial mutation operator is found to be most effective.

The objective of this work was to mainly consider the optimisation aspects of the DSAB damper placement problem. A number of related research directions need to be investigated in future, as listed below.

- (a) In this work, we have assumed all  $N_d$  dampers to have identical parameters (stiffness and damping coefficients). These parameters could also be added to the decision variables to give greater flexibility to the decision maker.
- (b) We have considered sets of two objective functions. For some problems, it may be desirable to consider three or four objective functions.
- (c) A systematic study of the effect of  $N_d$  on the best achievable objective values needs to be undertaken. As pointed out earlier [2],[13], a smaller number of dampers with optimal parameters and positions may be adequate to meet the desired specifications. Optimisation can be used to confirm this finding.
- (d) The present study could be extended to DSABs with larger  $N_d$  and  $N_f$ .

## Acknowledgement

This work was partially supported by the Science and Engineering Board (SERB), Department of science and technology (DST), Govt. of India. Financial support from DST in the form of Fund for Improvement of S&T Infrastructure (FIST) is also gratefully acknowledged. M.B.P. would like to thank Prof. Kumar Appaiah, IIT Bombay, for discussions related to programming aspects.

## References

- [1] D. De Domenico, G. Ricciardi, and I. Takewaki, "Design strategies of viscous dampers for seismic protection of building structures: a review," *Soil Dynamics and Earthquake Engineering*, vol. 118, pp. 144–165, 2019.
- [2] A. Bhaskararao and R. Jangid, "Seismic analysis of structures connected with friction dampers," *Engineering Structures*, vol. 28, no. 5, pp. 690–703, 2006.
- [3] C. Patel and R. Jangid, "Seismic response of dynamically similar adjacent structures connected with viscous dampers," *The IES Journal Part A: Civil & Structural Engineering*, vol. 3, no. 1, pp. 1–13, 2010.
- [4] S. Bharti, S. Dumne, and M. Shrimali, "Earthquake response of asymmetric building with mr damper," *Earthquake engineering and Engineering vibration*, vol. 13, no. 2, pp. 305–316, 2014.
- [5] M. Singh and L. Moreschi, "Optimal placement of dampers for passive response control," *Earthquake engineering & structural dynamics*, vol. 31, no. 4, pp. 955–976, 2002.
- [6] N. Wongprasert and M. Symans, "Application of a genetic algorithm for optimal damper distribution within the nonlinear seismic benchmark building," *Journal of Engineering Mechanics*, vol. 130, no. 4, pp. 401–406, 2004.
- [7] K.-S. Park, H.-M. Koh, and D. Hahm, "Integrated optimum design of viscoelastically damped structural systems," *Engineering Structures*, vol. 26, no. 5, pp. 581–591, 2004.
- [8] V. Matsagar and R. Jangid, "Viscoelastic damper connected to adjacent structures involving seismic isolation," *Journal of civil engineering and management*, vol. 11, no. 4, pp. 309–322, 2005.
- [9] M. Liu, S. Burns, and Y. Wen, "Multiobjective optimization for performance-based seismic design of steel moment frame structures," *Earthquake Engineering & Structural Dynamics*, vol. 34, no. 3, pp. 289–306, 2005.
- [10] K. Makita, R. Christenson, K. Seto, and T. Watanabe, "Optimal design strategy of connected control method for two dynamically similar structures," *Journal of Engineering Mechanics*, vol. 133, no. 12, pp. 1247–1257, 2007.
- [11] N. Lagaros and M. Papadrakakis, "Seismic design of rc structures: a critical assessment in the framework of multi-objective optimization," *Earthquake Engineering & Structural Dynamics*, vol. 36, no. 12, pp. 1623–1639, 2007.

- [12] O. Lavan and G. Dargush, "Multi-objective evolutionary seismic design with passive energy dissipation systems," *Journal of Earthquake Engineering*, vol. 13, no. 6, pp. 758–790, 2009.
- [13] K. Bigdeli, W. Hare, and S. Tesfamariam, "Configuration optimization of dampers for adjacent buildings under seismic excitations," *Engineering Optimization*, vol. 44, no. 12, pp. 1491–1509, 2012.
- [14] E. Aydin, "A simple damper optimization algorithm for both target added damping ratio and interstorey drift ratio," *Earthquakes and Structures*, vol. 5, no. 1, pp. 83–109, 2013.
- [15] M. Hadi and M. Uz, "Investigating the optimal passive and active vibration controls of adjacent buildings based on performance indices using genetic algorithms," *Engineering Optimization*, vol. 47, no. 2, pp. 265–286, 2015.
- [16] K.-S. Park and S.-Y. Ok, "Hybrid control approach for seismic coupling of two similar adjacent structures," *Journal of Sound and Vibration*, vol. 349, pp. 1–17, 2015.
- [17] M. Mastali, A. Kheyroddin, B. Samali, and R. Vahdani, "Optimal placement of active braces by using pso algorithm in near-and far-field earthquakes," *International Journal of Advanced Structural Engineering (IJASE)*, vol. 8, no. 1, pp. 29–44, 2016.
- [18] E. Aydin, B. Öztürk, and M. Dikmen, "Optimal damper placement to prevent pounding of adjacent structures considering a target damping ratio and relative displacement," *Omer Halisdemir University Journal of Engineering Sciences*, vol. 6, no. 2, pp. 581–592, 2017.
- [19] M. Barraza, E. Bojórquez, E. Fernández-González, and A. Reyes-Salazar, "Multi-objective optimization of structural steel buildings under earthquake loads using nsga-ii and pso," *KSCE Journal of Civil Engineering*, vol. 21, no. 2, pp. 488–500, 2017.
- [20] A. Bogdanovic and Z. Rakicevic, "Optimal damper placement using combined fitness function," *Frontiers in Built Environment*, vol. 5, p. 4, 2019.
- [21] H. Cetin, E. Aydin, and B. Ozturk, "Optimal design and distribution of viscous dampers for shear building structures under seismic excitations," *Frontiers in Built Environment*, vol. 5, p. 90, 2019.
- [22] A. Puthanpurayil, O. Lavan, and R. Dhakal, "Multi-objective loss-based optimization of viscous dampers for seismic retrofitting of irregular structures," *Soil Dynamics and Earthquake Engineering*, p. 105765, 2019.
- [23] H. Rahmani and C. Könke, "Seismic control of tall buildings using distributed multiple tuned mass dampers," *Advances in Civil Engineering*, vol. 2019, 2019.
- [24] S. Rajasekaran, *Structural Dynamics of Earthquake Engineering*. New Delhi: CRC Press, 2009.
- [25] K. Deb, A. Pratap, S. Agarwal, and T. Meyarivan, "A fast and elitist multiobjective genetic algorithm: NSGA-II," *IEEE Trans. Evol. Comput.*, vol. 6, no. 2, pp. 182–197, 2002.
- [26] C. A. C. Coello, G. T. Pulido, and M. S. Lechuga, "Handling multiple objectives with particle swarm optimization," *IEEE Trans. Evol. Comput.*, vol. 8, no. 3, pp. 256–279, 2004.
- [27] K. Deb, *Multi-objective Optimization Using Evolutionary Algorithms*. Chichester: J. Wiley and Sons, Ltd., 2009.